

## **Severe Weather in Texas and Louisiana on November 6, 2006 from 1700Z to 2100Z**

During the afternoon and early evening hours on Monday, November 6, 2006, residents of Louisiana and Texas prepared for a severe weather system that would bring drenching rains, lightning, and tornadoes into their neighborhoods. Satellite and radar imagery were useful in providing clues for thunderstorm development in Texas and for spotting potential hail and tornadoes in Louisiana. It is important to check cloud structures and types in visible, infrared, and water vapor satellite imagery because each image provides unique information about the storm system. In addition, radar images can be used to determine the precipitation intensity and wind velocities of particular thunderstorms.

Before delving into different images, it is important to first gain an overall sense of what is occurring in the atmosphere; assessing surface level maps is a great start in becoming familiar with the weather conditions present. Figure 1 depicts the 1800Z surface analysis for the continental United States. Interesting features displayed in this image include a dome of high pressure situated off of the coast of the Eastern Seaboard, low pressure located in the center of Arkansas, and a cold front draped into southeastern Texas.

The features present in the surface analysis can be seen in the visible satellite image. Figure 2 portrays visible satellite imagery of the eastern half of the United States at 1615Z. At this time, high pressure centered over the Eastern Seaboard is causing air at the surface to spin in an anti-cyclonic motion, producing easterly winds near eastern Florida. Meanwhile, the low pressure system in Arkansas is marching forward from the west; easterlies from the high pressure system and westerlies from the low pressure system are converging together in a path sweeping from the Gulf of Mexico through Mississippi and Alabama, causing instability and lift. From Figure 2, one can discern cirrus blow off from Illinois through Virginia. Beneath the cirrus are layers of mixed clouds consisting of stratocumulus (Illinois, Indiana, Missouri) and cumulonimbus (Arkansas, Louisiana, and Texas). In addition, a layer of fog is blanketing the middle of the country from Minnesota to eastern Texas. Of particular interest is convective development in southeast Texas: to the west of the Louisiana-Texas border, a line of thunderstorms is developing.

Visible imagery is produced when satellite radiometers capture and count how many photons are reflected back from the earth's features (such as clouds), and a computer puts together an image based on the data gathered from the radiometer. However, visible imagery is only available during the day when the sun's rays are being reflected off of the earth. In addition, one can infer different cloud heights when comparing features to one another, but cloud height cannot be directly determined from visible

satellite imagery. In order to determine the heights of particular clouds, it is best to use infrared satellite imagery. Figure 3 portrays infrared satellite imagery of the eastern continental United States at 1715Z. The infrared satellite image is produced by the satellite sensors that detect thermal (infrared) energy emissions radiated by the earth. Because clouds located higher up in the atmosphere are colder than clouds found near the surface, the higher clouds emit less heat (and thus less infrared radiation); they appear white on the infrared satellite image. Clouds found lower in the atmosphere (and near the surface, like fog) are warmer; they emit more heat (more infrared radiation) and appear darker on the infrared satellite image. In Figure 3, brighter clouds are found in the Gulf of Mexico and in Texas, Louisiana, Arkansas, Tennessee, and Illinois. In addition, brighter white clouds can be found in the west in states such as Montana, Wyoming, and Idaho. Lower clouds, such as stratus and fog, are found in a long path from Minnesota down to eastern Texas. When the infrared satellite imagery is allowed to loop, one can see that the low clouds sweeping from Montana to Texas dissipate from the outside inwards, which indicates that fog is burning off in these regions. Figure 4 shows the same infrared satellite imagery as Figure 3, but the cloud-top temperatures have been color coded so that it becomes much easier to distinguish between mid-level and higher-level clouds. According to the color key, the highest clouds occurring in Figure 4 are located in the Gulf of Mexico, with cloud-top temperatures of approximately  $-63^{\circ}\text{C}$ . In addition, cloud tops in Texas and Louisiana exhibit temperatures of approximately  $-55^{\circ}\text{C}$ , which are colder than the surrounding clouds; this means that the clouds in Texas and Louisiana are higher than the surrounding clouds, and thunderstorms with strong updrafts are developing in Texas and Louisiana.

Often, it is useful to observe areas of dry and moist air in order to determine whether storm systems should strengthen or decay. Figure 5 depicts enhanced water vapor satellite imagery at 1715Z. In this image, dark gray and bright orange areas denote dry air while light gray and white denote moist air. Bright white areas, such as the Gulf of Mexico, eastern Texas, and northern Louisiana, indicate where the atmosphere is saturated with water vapor. In addition to determining areas of dry and moist air, water vapor satellite imagery can be used to assess the development of the cyclone. In Figure 5, the cyclone's baroclinic leaf structure can be found over portions of Missouri, Indiana, Illinois, and Ohio (the continuation of the water vapor band into Pennsylvania and Maryland is due to blow off from the subtropical jet stream). In addition, dry air is beginning to intrude into the cloud head but has not completely wrapped into the center of the cloud head. Thus, cyclogenesis is occurring, but the cyclone has not yet reached maturity.

Interesting features, such as thunderstorm development in Texas, have been observed in each of the satellite images. The surface analysis for Texas, Oklahoma, Arkansas, and Louisiana at 1613Z can be found in Figure 6. The surface analysis portrays two interesting features occurring in Texas: in the northeastern portion of the state, fog is prevalent yet in the southeastern region it is absent. Line **1** in Figure 6 highlights the border between foggy and non-foggy areas. The presence of Line **1** is significant because it symbolizes a line of instability that can develop due to the fact that areas of fog remain cool during daytime hours while areas of clear skies increase in temperature due to diabatic heating from the sun. The fog/clear area temperature gradient can induce a pressure gradient that initiates convective development. In addition to the temperature gradient between the foggy and clear areas, a second temperature differential exists between northern and southern Texas, as represented by Line **2**. The presence of Line **2** is significant in that the temperatures behind the line are in the 50s and low 60s, whereas temperatures ahead of the line are in the high 60s to low 80s. Line **2** signals the presence of a cold front appended to the low pressure system (as depicted in Figure 1), and the temperature differential caused by the front aids in developing atmospheric instability in southeastern Texas.

The visible satellite imagery for the Texas, Oklahoma, Arkansas, and Louisiana area at 1701Z is found in Figure 7. Features of particular interest include cumulonimbi with overshooting tops extending from Mississippi to the coast of Texas, cirrus blow off from thunderstorms in northern Louisiana, and fog located in middle to lower Texas. In addition, two lines of convection can be detected in southern Texas, marked **A** and **B**. Convection line **A** is located in the vicinity of the fog/clear area line as depicted by Line **1** in Figure 6. Convection line **B** is located in the vicinity of the temperature gradient as depicted by Line **2** in Figure 6. When the visible imagery is allowed to loop, the fog located south of **A** burns off and thunderstorm development along Convection line **A** increases. Simultaneously, thunderstorms erupt near Convection line **B** due to the sea breeze flowing onto the Texas coast interacting with the temperature differential depicted in Line **2**. Figure 8 displays the visible satellite imagery for the same region as Figure 7, but for the time period of 2001Z. The fog that was south of **A** in Figure 7 has nearly burned off, and thunderstorms along Convective line **A** have grown due to the instability produced by the intersection of the fog/clear area differential heating line and the thunderstorms' gust fronts. In addition, Convective line **B** experienced increased thunderstorm growth due to the intersection of the cold front induced thermal gradient and a sea breeze coming in from the coast of Texas.

Determining the coldest cloud tops present requires looking at the infrared satellite image of the area. Figure 9 shows the enhanced infrared satellite imagery for Texas, Oklahoma, Arkansas, and

Louisiana at 1815Z. At this time, the coldest cloud tops are found in the Gulf of Mexico with temperatures of approximately  $-60^{\circ}\text{C}$ . Cloud top temperatures of approximately  $-40^{\circ}\text{C}$  can be found in eastern Texas and Louisiana. It is interesting to note that the first thunderstorms developing along Convective line A can be detected in this image. Figure 10 displays the enhanced infrared satellite imagery for the same region as Figure 9, but for 2031Z. Significant thunderstorm development is occurring in eastern Texas and eastern Louisiana as evident by the colder cloud tops (approximately  $-55^{\circ}\text{C}$  and  $-60^{\circ}\text{C}$ , respectively). Thunderstorm development in eastern Texas corresponds to Convective line A while development in eastern Louisiana corresponds to a passing prefrontal, warm sector squall line.

The precipitation intensity occurring with this storm system can be determined from the radar imagery. Figure 11 shows the radar imagery for the southeastern United States at 1814Z. In this image, a line of thunderstorms extends from Tennessee through Mississippi to southern Louisiana. When allowed to loop, the radar imagery indicates that the line of thunderstorms is a squall line with embedded self sustaining thunderstorms. Behind the squall line, a second band of high reflectivity precipitation is present. This secondary precipitation occurs because convection associated with the squall line has forced air parcels into the upper atmosphere, causing water vapor to condense into liquid water. Even though the squall line has passed through, gravity overcomes the buoyancy force on residual hydrometeors in the upper atmosphere, and they fall to the ground as a band of higher reflectivity precipitation.

Intensification of the cold-front-induced squall line is evident in Figure 12, in which the thunderstorms in southern Mississippi through Louisiana have organized into a single band. The most intense precipitation rate occurred in eastern Louisiana with a reflectivity value of approximately 60 dBz. It is interesting to note that convective development along Convective line C is producing relatively intense precipitation with reflectivity values of approximately 50 dBz. Figure 13 depicts the radar imagery from New Orleans, Louisiana, at 1942Z. In this image, thunderstorms moving from a southerly direction are converging with the cold front induced thunderstorms moving in from the west. As the southerly thunderstorms dissipate, their gust fronts are being incorporated into the development of the cold-front-induced thunderstorms.

In order to determine the wind speeds and directions associated with particular thunderstorms, the storm relative velocity mode of the radar is used. Figure 14 shows the radar imagery in storm relative velocity mode for the line of thunderstorms near New Orleans, Louisiana, at 2029Z. An interesting feature present in Figure 14 is an area near Baton Rouge in which winds moving

approximately 30 knots away from the radar (orange) are surrounded by winds moving approximately 10 to 22 knots towards the radar (green). Figure 15 allows for a closer view of the wind “couplet.” Although the radar indication of a tornado is the presence of a couplet (a microscale region in which high velocity winds moving towards the radar are adjacent to high velocity winds moving away from the radar), the feature found in Figures 14 and 15 does not seem to be a couplet because the winds moving away from the radar are surrounded (as opposed to being adjacent) with winds moving towards the radar. Thus, the radar feature may depict a microburst: an incredibly strong downdraft that is less than 2.5 miles wide which has made impact with the ground, forcing the air to deflect to each direction. However, in the interest of public safety, a National Weather Service (NWS) forecaster should submit a tornado warning in order to allow the public enough time to prepare in case the feature was indeed a tornado.

A particular radar feature that is useful in predicting hail is the vertically integrated liquid (VIL) mode. Figure 16 depicts the VIL for eastern Louisiana at 2028Z. The VIL is the integration of reflectivity within a column of air, and it represents the amount of precipitation within the air column. The higher the VIL value, the greater amount of water is present in the air column and the higher probability that hail is present. In Figure 16, the radar image indicates that an area southeast of Baton Rouge is exhibiting a VIL value of approximately  $45 \text{ kg m}^{-2}$ , while surrounding areas are exhibiting much lower values of approximately 1 to  $30 \text{ kg m}^{-2}$ . Although high values of VIL cannot guarantee the presence of hail, it does signify that there is sufficient moisture within the thunderstorms to produce hail. Thus, NWS forecasters spotting this feature should be on the alert to submit a severe thunderstorm warning for locations in the path of the storm.

In order to verify the identification of tornadoes and hail on satellite and radar imagery, it is useful to compare observed features from imagery with storm reports gathered from the areas experiencing the observed weather. Figure 17 shows the Storm Prediction Center’s storm reports for 6 November 2006. According to the Storm Prediction Center (SPC), at 2110Z the sheriff’s office of St. Tammany, Louisiana reported that residents observed flying debris and snapping trees in evidence of a tornado. Although the reported SPC time is one hour later than the time depicted in figures 14 and 15, it is likely that it took about an hour for St. Tammany residents to contact the sheriff and for the sheriff to contact the SPC. In addition, the location of St. Tammany with respect to Baton Rouge, Louisiana is consistent with the location of the “couplet” structure with respect to Baton Rouge in Figure 15. Thus, it is possible that the feature found in Figure 15 was indeed a tornado: although the feature present is not a

classic tornadic couplet, it did indicate that significant shear was present in the storm which is necessary for tornado development.

As evident in this case study, many different types of imagery are available to forecasters who are on the alert for severe weather. From visible, infrared, and water vapor satellite images, one can gather a plethora of information about a cyclone's development and the location of convective instability. Radar images are useful, too, in providing clues about the availability of hail and the presence of wind shear. Best of all, satellite and radar imagery can augment weather map analysis to help give forecasters obtain a better understanding of the state of the atmosphere.

## Reference

Storm Prediction Center. *SPC Storm Reports for 11/06/06*. U.S. Department of Commerce, National Oceanographic and Atmospheric Administration, Storm Prediction Center; November 2006.

<[http://www.spc.noaa.gov/climo/reports/061106\\_rpts.html](http://www.spc.noaa.gov/climo/reports/061106_rpts.html)>

## Appendix

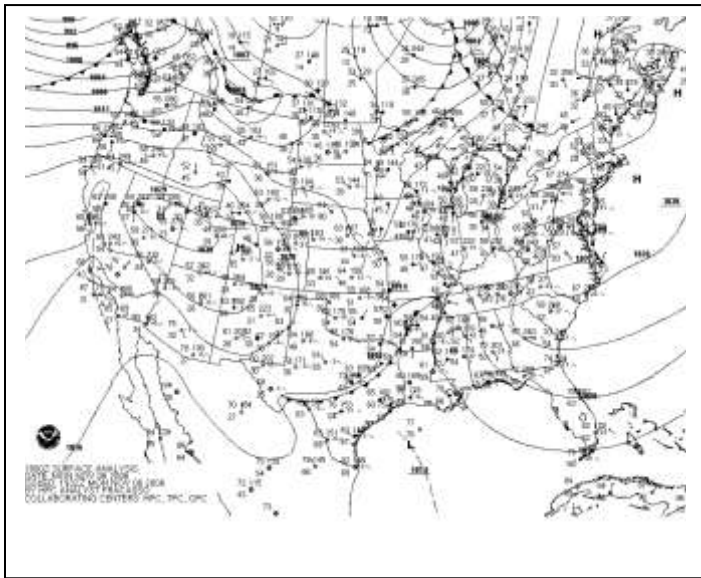


**Figure 1: Surface Analysis for the continental United States at 1800Z on 6 November 2006.** *Courtesy of the National Weather Service*

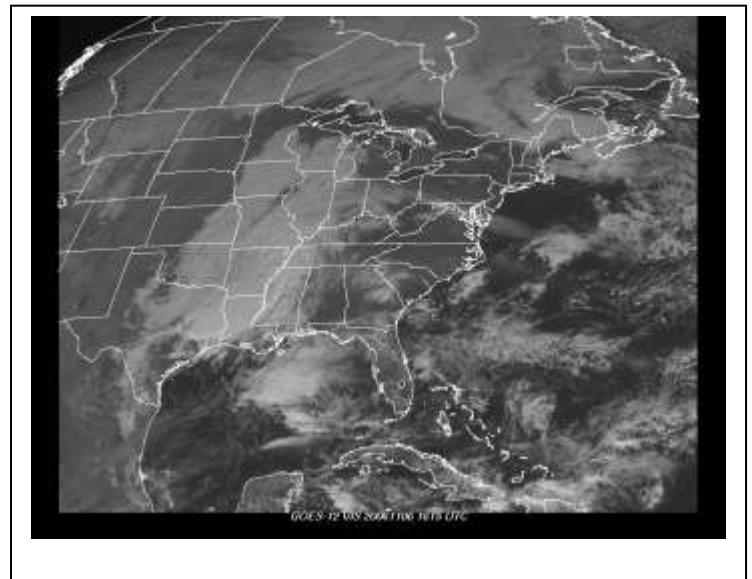


**Figure 2: Visible satellite imagery from GOES-12 at 1615Z on 6 November 2006.** *Courtesy of the Ohio State University Atmospheric Sciences Program*

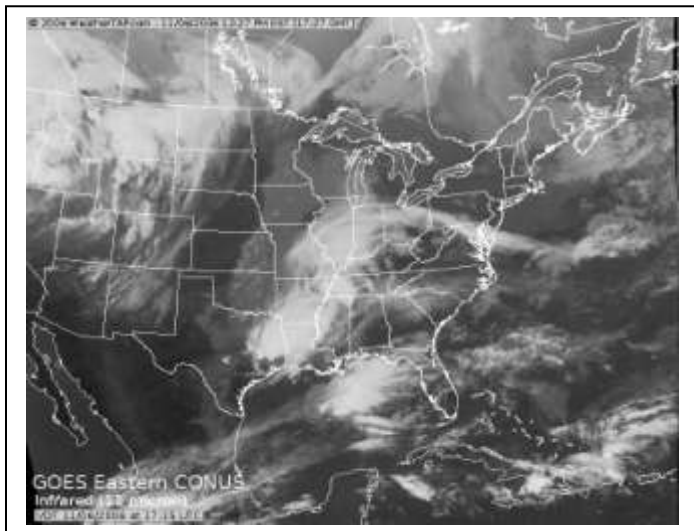


**Figure 3: Infrared satellite imagery from GOES-12 at 1715Z on 6 November 2006.** *Courtesy of WeatherTAP.com*



**Figure 4: Enhanced infrared satellite imagery from GOES-12 at 1715Z on 6 November 2006.** *Courtesy of WeatherTAP.com*

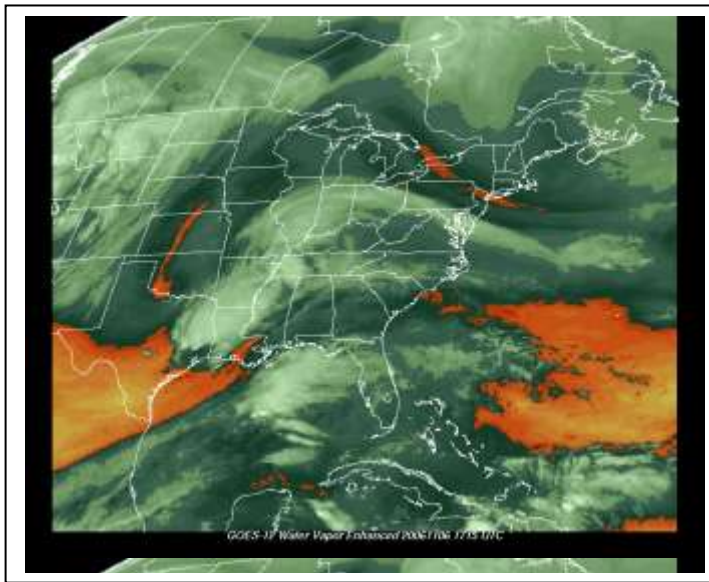


**Figure 5: Enhanced water vapor satellite imagery from GOES-12 at 1715Z on 6 November 2006. The letter A represents the baroclinic leaf structure, and the letter B represents the cloud head. Courtesy of the Ohio State University Atmospheric Sciences Program**

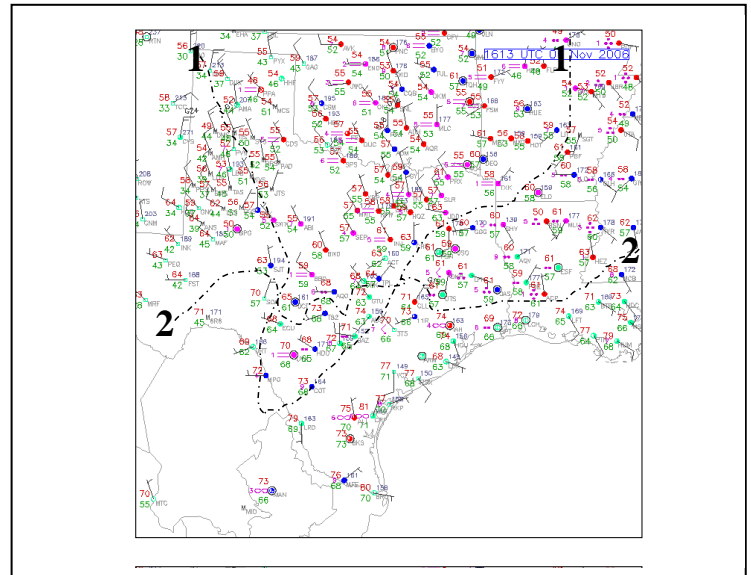


**Figure 6: Surface Analysis of Texas, Oklahoma, Arkansas, and Louisiana at 1613Z on 6 November 2006. Line 1 denotes the border between foggy and non-foggy areas. Line 2 indicates the presence of a cold front. Courtesy of the Ohio State University Atmospheric Sciences Program**

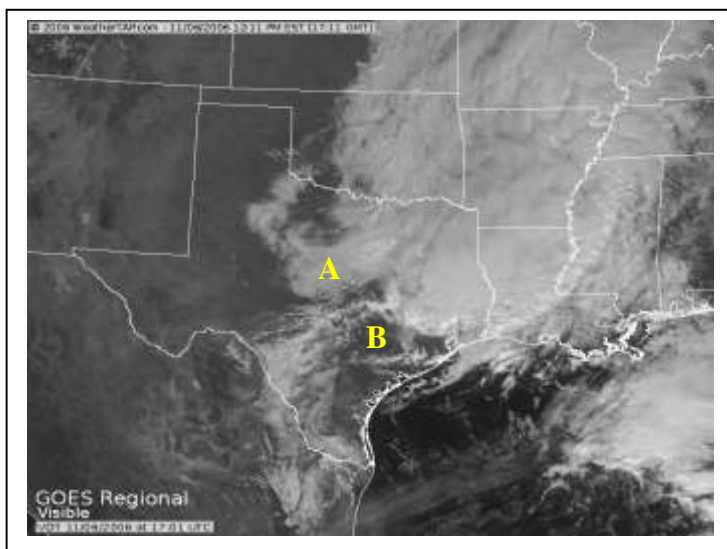


**Figure 7: Visible satellite imagery from GOES-12 at 1701Z on 6 November 2006. Convection line A is located near the fog/clear area line as depicted by Line 1 in Figure 6. Convection line B is located near the temperature gradient as depicted by Line 2 in Figure 6. Courtesy of WeatherTAP.com**

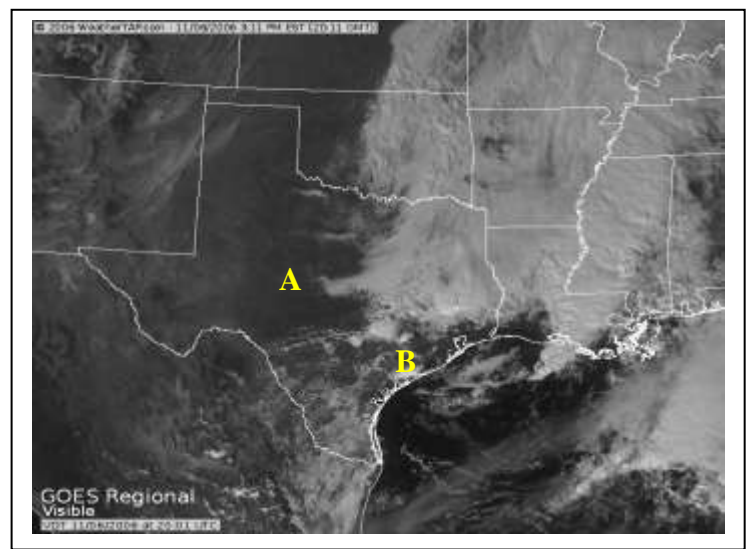


**Figure 8: Visible satellite imagery from GOES-12 at 2001Z on 6 November 2006. Development along Convection line A occurs due to fog burn off, and development along Convection line B occurs due to a sea breeze interacting with the temperature differential depicted in Figure 6. Courtesy of WeatherTAP.com**

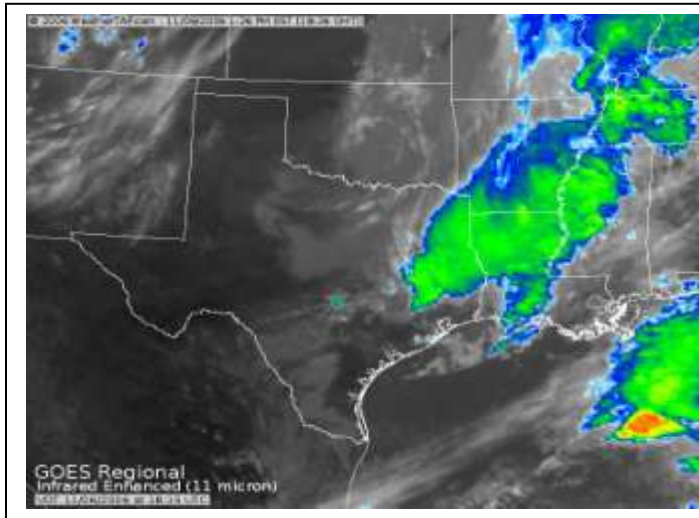


**Figure 9: Enhanced infrared satellite imagery from GOES-12 at 1815Z on 6 November 2006. Courtesy of WeatherTAP.com**

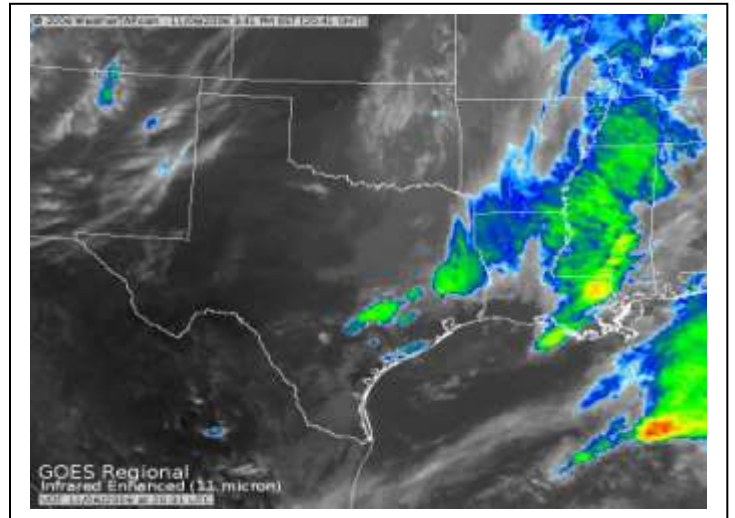


**Figure 10: Enhanced infrared satellite imagery from GOES-12 at 2031Z on 6 November 2006. Courtesy of WeatherTAP.com**



**Figure 11: Radar imagery for the southeastern US at 1814Z on 6 November 2006. Courtesy of WeatherTAP.com**

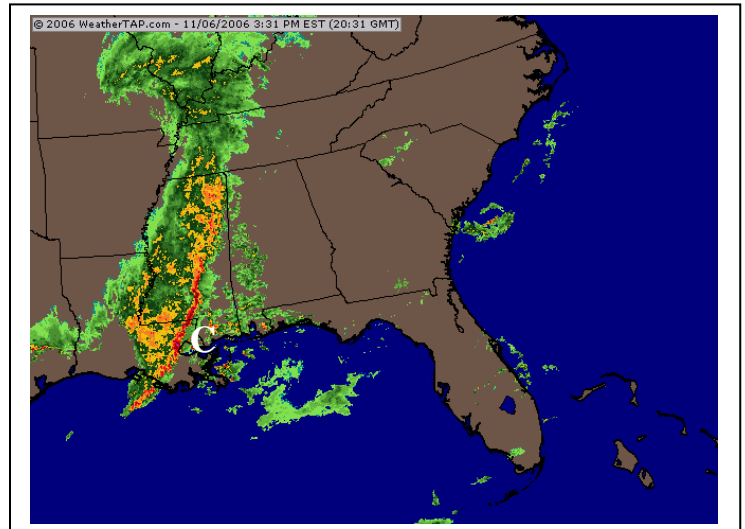


**Figure 12: Radar imagery for the southeastern US at 2031Z on 6 November 2006. Precipitation reflectivity values associated with the thunderstorms along Convective line C approach the severe threshold of 50 dBz. Courtesy of WeatherTAP.com**

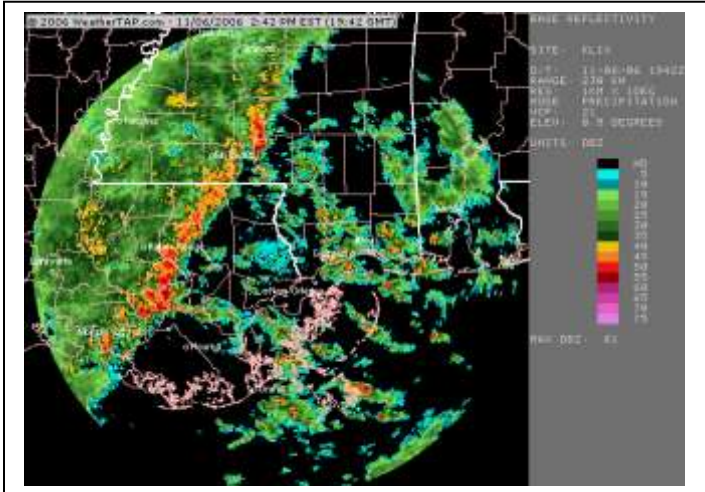


Figure 13: Radar imagery for eastern Louisiana at 1942Z on 6 November 2006. Courtesy of WeatherTAP.com

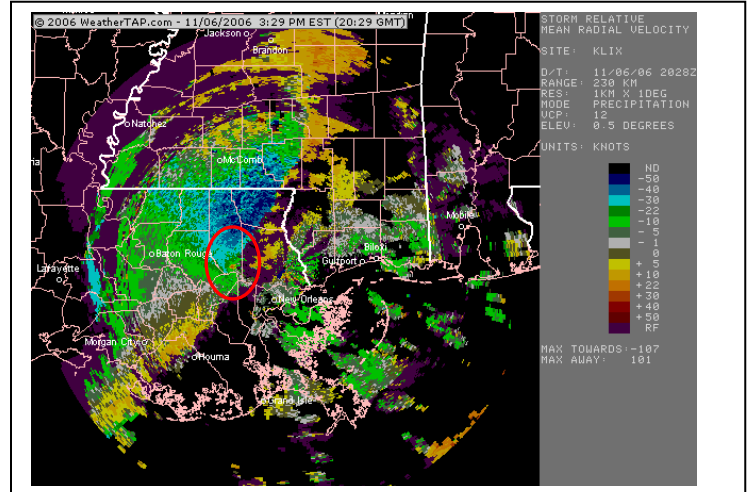


Figure 14: Radar imagery (Storm Relative Velocity mode) for eastern Louisiana at 2029Z on 6 November 2006. A couplet is present within the red oval. Courtesy of WeatherTAP.com

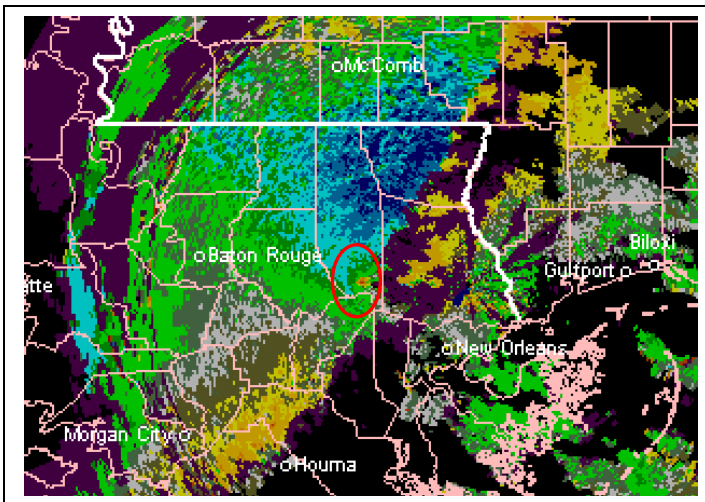


Figure 15: A closer view of the radar feature found in Figure 14. Courtesy of WeatherTAP.com

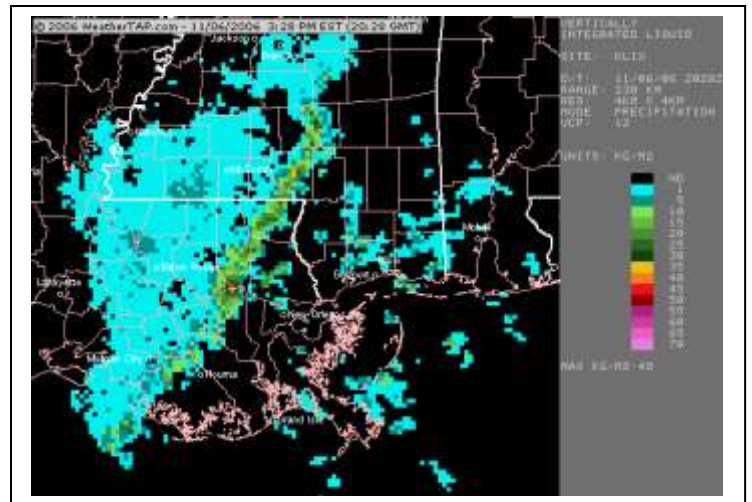


Figure 16: Radar imagery (Vertically Integrated Liquid mode) for eastern Louisiana at 2028Z on 6 November 2006. Courtesy of WeatherTAP.com

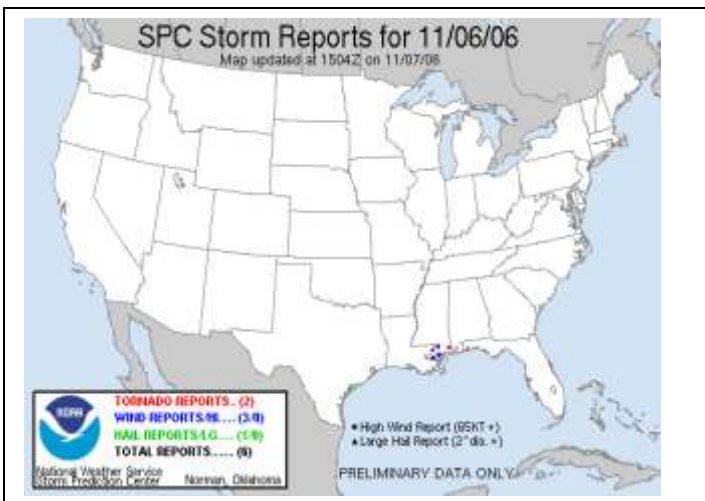


Figure 17: SPC Storm Reports for 6 November 2006. Courtesy of the Storm Prediction Center